ELECTROMAGNETIC WAVE SCATTERING

Electromagnetic wave scattering is the reradiation of electromagnetic energy that results when an electromagnetic field encounters an abrupt change in electrical parameters. Typically, this occurs when an electromagnetic field is incident on a structure or scattering object. When the original electromagnetic field crosses the boundary between two regions of different material, each with different electrical properties, the field will change as it enters the second region. Sources, including conduction, displacement, and polarization currents, will be induced at the discontinuity between the two regions. These currents act as sources of electromagnetic radiation, much like the sources of the original incident electromagnetic field. This reradiation is called electromagnetic scattering, because it scatters the incident electromagnetic field from its original propagation path.

TYPES OF ELECTROMAGNETIC SCATTERING

Fundamentally, there are three types of electromagnetic scattering mechanisms: reflection, refraction, and diffraction. These scattering mechanisms can radiate specularly or diffusely. Specular scattering means that electromagnetic reradiation travels in parallel rays. Diffuse scattering means the spreading of the electromagnetic field as it propagates away from the scattering object.

Specular Scattering

Of the three fundamental scattering mechanisms, the most familiar are specular reflection and refraction. If any corners or bends that exist at the boundary are very gradual compared to the wavelength of the incident field, then the boundary tends to cause *specular* scattering. Optical scattering is often assumed to be specular, because most obstructing bodies are electrically large compared to optical wavelengths. Specular scattering can be modeled with the specular law of reflection and Snell's law of refraction.

Specular Reflection. A familiar example of specular reflection is the common reflection of a visible image in a mirror, since the dimensions of the mirror are huge compared to the wavelength of visible light. The ratio of the reflected field to the incident field strength is called the reflection coefficient Γ.

Refraction. The energy that is not reflected from the electrically large boundary is transmitted through the boundary. The ratio of the transmitted field strength to the incident field strength is called the transmission coefficient T. In the process of propagating from one electrical medium to the next,

the speed of propagation changes. This change in speed causes a change in the propagation angle at the boundary. This phenomenon is commonly seen with visible light at the surface of a calm pool of water. The fact that an object extending from the air into the water appears bent is due to the increase in the propagation velocity of light as it leaves the water and enters the air. This phenomenon can be modeled with Snell's law of refraction.

Diffuse Scattering

The laws for specular scattering are only valid for electrically large scattering bodies. If the object causing the electromagnetic scattering is small compared to the wavelength of the incident electromagnetic field, the induced currents would tend to bend around the contour, creating *diffuse* scattering. Unlike specular scattering, diffuse scattering results when the electromagnetic energy spreads out as it radiates from the scattering object. The smaller the object, the more the energy will spread as it reradiates.

A simple example of diffuse scattering is an electromagnetic field incident upon a cylindrical conductor of small radius, where the electric field is parallel to the axis of the cylinder. At frequencies below the microwave region of the electromagnetic spectrum, a thin copper wire will have an electrically small radius. A first approximation is to assume that the current that is induced by the incident field is uniformly distributed across the entire cross section of the wire. The scattered or reradiated field from this wire is similar to the field radiated from a wire antenna having the same linear current distribution. However, the total field around the wire is the superposition, or vector sum, of the scattered field and the original incident field that would have existed without the wire present. The scattered field, added to the incident field, creates a pattern with constructive reinforcement in some directions and destructive cancellation in other directions. This is the function of the passive elements found on the Yagi–Uda antenna, common in television and other VHF and UHF communications.

In the Yagi–Uda antenna, only one set of elements is active. The active (or driven) element usually makes up a half-wavelength dipole antenna. The other elements are simply conductive cylinders or wires that reradiate some of the energy incident on them from the active element. Depending on the relative lengths of these passive elements, each of their radiated fields will add to the incident field of the active element, to create an overall pattern of power flow (1) This focusing of energy is called antenna gain. Other forms of diffuse scattering by electrically small bodies are not so intentional.

Diffuse Diffraction

Another form of scattering, which cannot be accounted for by reflection or refraction, is diffraction. For electrically large scattering bodies, diffraction appears to occur at geometrical discontinuities such as edges and corners. A first approximation is that currents induced only at these discontinuities reradiate electromagnetic energy. Diffraction is the scattering mechanism that accounts for radiation filling in the region that would have been completely blocked (shadowed) by an opaque obstruction.

Diffraction and reflection are important scattering mechanisms in communications. Whether in an urban or rural environment, a cell-phone user rarely has a direct line of sight to the cell base station. Often, the communication link can only be established due to energy reflecting off of a nearby building, or energy diffracted around a building or over a hill. Since typically, these obstructions are electrically large, ray-tracing techniques, which incorporate the laws for specular reflection and diffuse diffraction at edges, are often used to model the propagation characteristics of the communication channel.

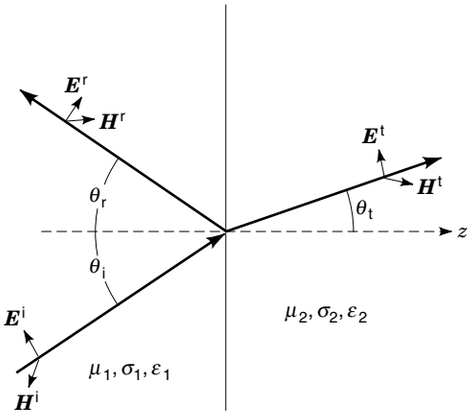

Figure 1. Illustration of Snell's law. A plane-wave electromagnetic field obliquely incident onto a plane boundary, separating medium 1 (μ_1, ϵ_1, σ_1) from medium 2 (μ_2, ϵ_2, σ_2). A reflected field and a transmitted field scatter from this discontinuity in electrical constants.

THE LAWS OF SPECTRAL REFLECTION AND REFRACTION

In many applications, an electromagnetic field can be assumed to be a plane wave. A plane wave is a convenient approximation amounting to the assumption that the electromagnetic field does not vary over the plane perpendicular to the direction of propagation. This approximation is similar to assuming that over small geographic areas the Earth is flat. For wave propagation, this assumption is valid for a small observation area at a great distance from the source of a spherically propagating wave.

Figure 1 shows a plane-wave electromagnetic field incident on a boundary in the xy plane. The generalized electric field will have components in the x, y, and z directions, that is,

$$\boldsymbol{E} = (\hat{\boldsymbol{x}}E_x + \hat{\boldsymbol{y}}E_y + \hat{\boldsymbol{z}}E_z)e^{-j\beta(\sin\theta_i x + \cos\theta_i z)} \tag{1}$$

where $\beta = \omega\sqrt{\mu\epsilon}$ is the phase constant or wave number in radians per meter, μ is the permeability in henrys per meter, and ϵ is the permittivity of the material in farads per meter. Imposing the tangential boundary condition for the electric field, the sum of the tangential components of the incident and reflected fields must be equal to that of the transmitted field (2–4),

$$(\hat{\boldsymbol{x}}E_x^i + \hat{\boldsymbol{y}}E_y^i)e^{-j\beta_1 \sin\theta_i x} + (\hat{\boldsymbol{x}}E_x^r + \hat{\boldsymbol{y}}E_y^r)e^{-j\beta_1 \sin\theta_r x} = (\hat{\boldsymbol{x}}E_x^t + \hat{\boldsymbol{y}}E_y^t)e^{-j\beta_2 \sin\theta_t x} \tag{2}$$

This equality can only be true for all x when the exponents, or phases, are equal:

$$\beta_1 \sin \theta_i x = \beta_1 \sin \theta_r x = \beta_2 \sin \theta_t x \tag{3}$$

Equation (3), proves the well-known specular law for reflection (5),

$$\theta_i = \theta_r \tag{4}$$

which simply states that the angle of reflection equals the angle of incidence. Equation (3) also leads to Snell's law of refraction,

$$\frac{\sin \theta_i}{\sin \theta_t} = \sqrt{\frac{\mu_2 \epsilon_2}{\mu_1 \epsilon_1}} \tag{5}$$

For most material, the permeability is the same as that of free space, $\mu = \mu_0$. Assuming $\mu_1 = \mu_2$, Eq. (5) reduces to

$$n_1 \sin \theta_1 = n_2 \sin \theta_2$$

where $n = \sqrt{\epsilon_r}$ is the index of refraction and ϵ_r is the relative permittivity or dielectric constant.

ELECTROMAGNETIC THEOREMS

Many electromagnetic scattering problems do not lend themselves to the simple application of the laws of reflection and refraction. To develop more sophisticated analysis tools, a discussion of some basic electromagnetic theorems will be useful.

Uniqueness Theorem

Knowledge of the sources induced on the surface of a scattering body S enables unique solutions of the fields reradiated by those induced sources. Conversely, the known fields allow a unique calculation of the induced sources. The electric field $\boldsymbol{E}$ and magnetic field $\boldsymbol{H}$ are uniquely determined if (6,7)

1. $\hat{\boldsymbol{n}} \times \boldsymbol{E}$, the tangential component of $\boldsymbol{E}$, is specified on S,
2. $\hat{\boldsymbol{n}} \times \boldsymbol{H}$, the tangential component of $\boldsymbol{H}$, is specified on S, and
3. $\hat{\boldsymbol{n}} \times \boldsymbol{E}$ is specified on part of S, and $\hat{\boldsymbol{n}} \times \boldsymbol{H}$ is specified on the remaining part of S.

Induction Theorem

In general, sources, such as conduction, displacement, and polarization currents, are induced at electrical discontinuities in the medium through which the incident field is propagating. Figure 2 shows a typical discontinuity represented by region 2. Region 2 represents a scattering body of material consisting of a different permittivity ϵ, permeability μ, and conductivity σ, than those of the surrounding region 1. Region 2 is bounded by a surface S. Assume that an electric field, $\boldsymbol{E}_1$, and its associated magnetic field $\boldsymbol{H}_1$, originate from a source current density $\boldsymbol{J}_0$. This source could simply be the current oscillating in a transmitting antenna. These fields propagate undisturbed, through region 1, until they become incident upon the scattering body of region 2. As the fields cross the boundary between region 1 and region 2, they will be perturbed, that is, $\boldsymbol{E}_2$ and $\boldsymbol{H}_2$ in region 2 will generally not be equal to the fields $\boldsymbol{E}_1$ and $\boldsymbol{H}_1$ propagating in region 1. This abrupt change or discontinuity in electric and magnetic field strength results in currents that are induced at the discontinuity. In general these currents will be distributed through the volume of regions 1 and 2, depending on their electrical constants.

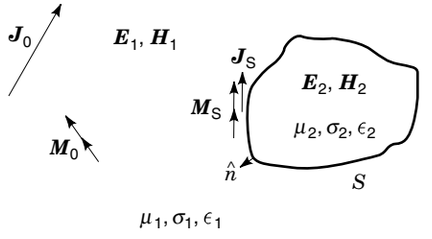

Figure 2. A scattering body. The incident field propagates from the source current, $\boldsymbol{J}_0$, through region 1. As this field strikes region 2, the currents $\boldsymbol{J}_s$ and $\boldsymbol{M}_s$ are induced at the surface S of the scattering body.

According to the induction theorem, whenever there is a discontinuity of the $\boldsymbol{E}$ and $\boldsymbol{H}$ fields crossing a boundary S between two media with different electrical constants, one can assume that induced currents at S cause the discontinuities in the fields. The induced current can be an electric current sheet (6–8)

$$\boldsymbol{J}_s = \hat{\boldsymbol{n}} \times (\boldsymbol{H}^s - \boldsymbol{H}^t) = -\hat{\boldsymbol{n}} \times \boldsymbol{H}^i \tag{6a}$$

or a fictitious, but mathematically useful magnetic current sheet

$$\boldsymbol{M}_s = -\hat{\boldsymbol{n}} \times (\boldsymbol{E}^s - \boldsymbol{E}^t) = \hat{\boldsymbol{n}} \times \boldsymbol{E}^i \tag{6b}$$

The superscripts i, s, and t pertain to the incident, outwardly scattered (reflected), and transmitted fields, respectively, and $\hat{\boldsymbol{n}}$ is the normal unit vector pointing out of the scattering body. If the scattering object is a perfect conductor, the transmitted fields vanish, leaving

$$\boldsymbol{J}_s = -\hat{\boldsymbol{n}} \times \boldsymbol{H}^i = \hat{\boldsymbol{n}} \times \boldsymbol{H}^s \tag{7a}$$

and

$$\boldsymbol{M}_s = \hat{\boldsymbol{n}} \times \boldsymbol{E}^i = -\hat{\boldsymbol{n}} \times \boldsymbol{E}^s \tag{7b}$$

The induction theorem alleviates the problem of knowing the exact distribution of current densities throughout the volume of the scattering body. The assumed currents exist only on the boundary S between the two media. Furthermore, the induced currents can be calculated directly from knowledge of the incident field that would have existed in the absence of any scattering object.

Equivalence Principle

If two different sources produce the same radiating field within a region, these sources are equivalent (8). If both regions have the same electrical constants, only an inwardly scattered (transmitted) field exists. It follows from Eq. (6) that the fields that are incident on the boundary S can be replaced by the equivalent current sheets

$$\boldsymbol{J}_s = \hat{\boldsymbol{n}} \times \boldsymbol{H}^s = \hat{\boldsymbol{n}} \times \boldsymbol{H}^i \tag{8a}$$

and

$$\boldsymbol{M}_s = -\hat{\boldsymbol{n}} \times \boldsymbol{E}^s = -\hat{\boldsymbol{n}} \times \boldsymbol{E}^i \tag{8b}$$

where in this case, $\hat{\boldsymbol{n}}$ is pointing in the direction of the transmitted or scattered wave. The equivalence theorem is useful for modeling radiation through apertures, such as a slot in a conductive plane or a horn antenna.

DIFFRACTION

Diffraction is the scattering mechanism that neither reflects off nor transmits through a structure. Even with opaque structures, allowing no transmission, diffraction accounts for radiation into the geometrical shadow region. This scattering mechanism cannot be modeled with Snell's law. To analyze diffraction exactly would require more knowledge about the induced current distribution around the scattering structure than would typically be available. Therefore approximations must be made to simplify the analysis. Two common approaches to analyzing diffraction are the use of geometrical optics and physical optics.

Geometrical Optics

Geometrical optics (GO) is a ray-tracing technique that assumes that the electromagnetic energy travels in straight parallel lines, or *rays,* that are perpendicular to the wavefront. These rays travel from the point of reradiation to the observation point. While relatively easy to implement (9,10), GO is an approximation that relies on some important assumptions, primarily that the wavelength of the electromagnetic field must approach zero. Clearly, GO is an asymptotic technique only valid for sufficiently high frequencies, such that the wavelength is small compared to the dimension of the obstruction. Since GO assumes infinite frequency, it ignores the wave nature of the electromagnetic scattering field, thus ignoring diffraction. The GO model creates an abrupt change in energy at the transition from the illuminated region to the shadow region. The abrupt change in field strength, without currents or charges to account for this discontinuity, violates boundary conditions. Therefore, GO provides only the crudest model, accounting only for reflection and refraction, but not for diffraction.

The geometrical theory of diffraction (GTD) extends GO to account for diffraction, by introducing a diffraction coefficient, D, analogous to Γ for reflection and to T for transmission (11–13). The total electric field $\boldsymbol{E}^T$ around the obstruction is

$$\boldsymbol{E}^T = \boldsymbol{E}^g + \boldsymbol{E}^d \tag{9}$$

where $\boldsymbol{E}^g$ is the electric field predicted by GO and is zero in the shadow region. The diffracted field for a plane wave of incidence is given by (14)

$$\boldsymbol{E}^d(r) = D\boldsymbol{E}_0 \frac{e^{-j\beta r}}{\sqrt{r}} \tag{10}$$

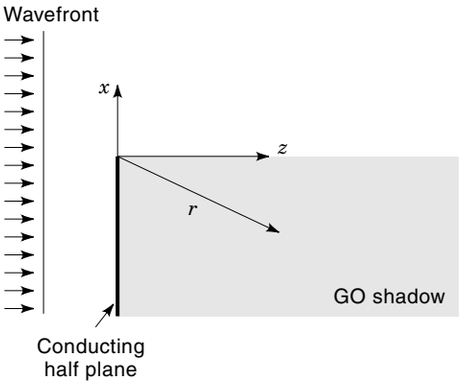

Figure 3. Half-screen diffraction using the GTD. The currents induced at the edge of the conducting half screen radiate into the GO shadow region.

Figure 3 shows a plane wave incident on a perfectly absorbing half screen. The diffraction coefficient can be quite involved, even for this simple scattering structure. However, away from the shadow boundary (15),

$$\boldsymbol{E}^d = -\tfrac{1}{2}\boldsymbol{E}_0 \frac{\sqrt{\lambda r}}{\pi x} e^{-j\beta r} \tag{11}$$

In the shadow ($-x$), the diffracted field given in Eq. (11) is the only field present. In the region of GO illumination ($+x$), the magnitude of the diffracted field of Eq. (11) subtracts from the incident field. Figure 4 illustrates the sum of the diffracted field and the GO incident field for (a) $z = 2\lambda$ and (b) $z = 20\lambda$. Clearly, there is a discontinuity at the transition between the GO illumination and shadow regions, around $x = 0$. This is an obvious limitation of the GTD, since there should be a smooth transition. One crude solution would be to simply draw a smooth curve connecting each side of the discontinuity through the point $x = 0$, $E = E_0/2$. A more sophisticated method is the uniform theory of diffraction (UTD), which is an extension of the GTD that forces a smooth transition between the GO illumination and shadow boundary (16).

Many common diffraction problems, such as hilltops and buildings, can be modeled with this half-screen or knife-edge approximation. However, the GTD still relies on several assumptions. The diffracted ray is assumed to depend entirely on the incident ray and the characteristics of the discontinuity itself, such as an edge of a scattering structure (17). The GTD is still a high-frequency asymptotic approximation, because it assumes that the structure is electrically large and conductive (18). Furthermore, the GTD suffers from the unrealistic discontinuity problem at the GO illumination–shadow boundary.

Physical Optics

The edge-diffraction problem of Fig. 3 can also be analyzed using the concept of physical optics (PO), which relies on Huygens' principle. Huygens' principle states that each point of a primary wavefront acts as a secondary point source. Each of these secondary sources radiates a spherical wave (14). The primary difference between PO and the GTD is that the GTD assumes rays connect from the geometrical discontinuity to

the observation point, while PO assumes that secondary spherical waves radiate from the unobstructed primary wavefront. Figure 5 shows Huygens sources radiating into the GO shadow region behind the absorbing half screen. The elementary electric field due to each secondary point source is

$$d\boldsymbol{E} = \frac{\boldsymbol{E}_0}{r+\delta}\, e^{-j\beta(r+\delta)} \tag{12}$$

where r is the distance from the observation point to the conducting half plane, and δ is the additional distance to the secondary sources. From Fig. 5,

$$(r+\delta)^2 = r^2 + 2r\delta + \delta^2 = x^2 + r^2 \tag{13}$$

Clearly, the secondary sources closest to the half screen will dominate the amplitude term in Eq. (12). Therefore, one can make the assumption that $r \gg \delta$ in the amplitude term, and

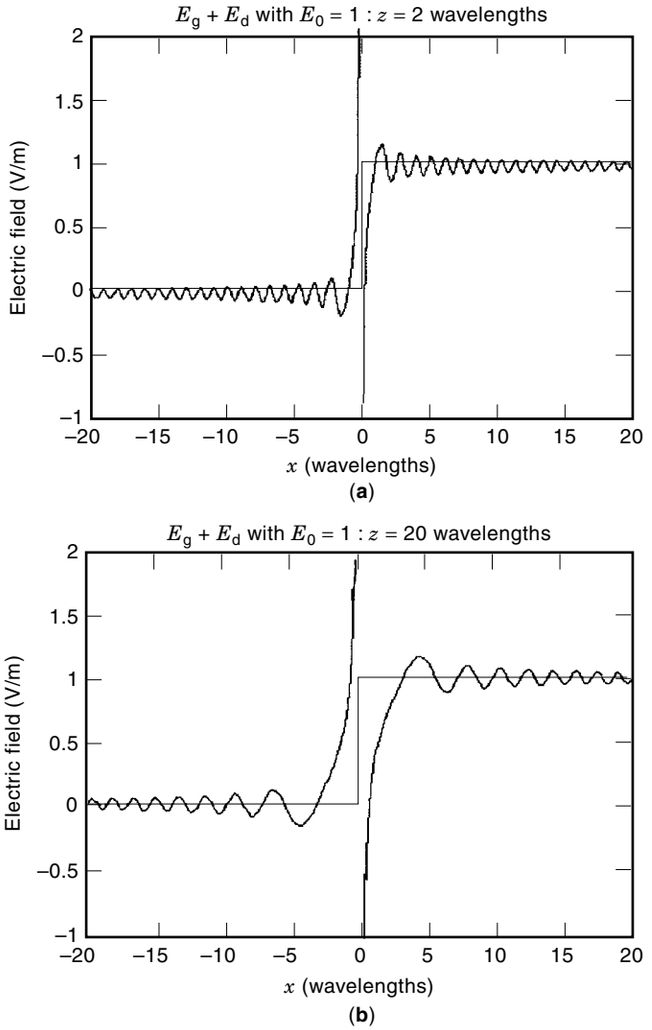

Figure 4. Simulation of half-screen diffraction by the GTD. The solid straight line represents the GO incident field. The oscillating curve is the diffracted field, calculated by the GTD, added to the GO field, at a distance behind the screen of (a) $z = 2$ wavelengths and (b) $z = 20$ wavelengths.

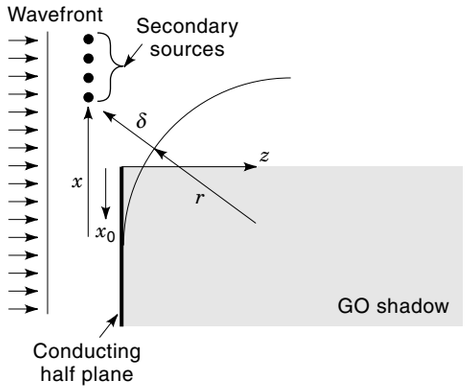

Figure 5. Half-screen diffraction using PO. The unblocked secondary sources radiate into the GO shadow region, accounting for diffraction.

$r^2 \gg \delta^2$ for the phase term. Thus, Eq. (13) reduces to

$$\delta = \frac{x^2}{2r} \tag{14}$$

and Eq. (12) becomes

$$\boldsymbol{E} = \boldsymbol{E}_0 / r\, e^{-j\beta r} \int_{x_0}^{\infty} e^{-j\beta x^2/2r}\, dx \tag{15}$$

where r is a constant. Letting $u = \sqrt{2/\lambda r}\, x$ and $u_0 = \sqrt{2/\lambda r}\, x_0$, Eq. (15) becomes

$$\boldsymbol{E} = \sqrt{\frac{\lambda}{2r}}\, \boldsymbol{E}_0 e^{-j\beta r} \int_{u_0}^{\infty} e^{-j\pi u^2/2}\, du \tag{16}$$

The limits of integration can be split into two terms:

$$\boldsymbol{E} = \sqrt{\frac{\lambda}{2r}}\, \boldsymbol{E}_0 e^{-j\beta r} \left(\int_0^{\infty} e^{-j\pi u^2/2}\, du - \int_0^{u_o} e^{-j\pi u^2/2}\, du \right) \tag{17}$$

which has the form of Fresnel cosine and sine integrals. Equation (17) can be written as

$$\boldsymbol{E} = \sqrt{\frac{\lambda}{2r}}\, \boldsymbol{E}_0 e^{-j\beta r} \left\{ \tfrac{1}{2} + j\tfrac{1}{2} - [C(u_0) + jS(u_0)] \right\} \tag{18a}$$

where $C(u_0)$ and $S(u_0)$ are the Fresnel sine and cosine integrals respectively (19–21). The solution to Eq. (18a) is similar to the GTD solution for Fig. 3, with the exception that Eq. (18a) for PO does not suffer the discontinuity of Eq. (11) for GTD. In fact, Eq. (18a) has an analytic solution in the GO illumination–shadow transition region. The total electric field at $x_0 = 0$ is

$$\boldsymbol{E}(x_0 = 0) = \sqrt{\frac{\lambda}{2r}}\, \boldsymbol{E}_0 e^{-j\beta r} \left(\tfrac{1}{2} + j\tfrac{1}{2} \right) \tag{18b}$$

and has a magnitude of $(\boldsymbol{E}_0/2)\sqrt{\lambda/r}$.

DIFFRACTION THROUGH AN APERTURE

The equivalence principle can be combined with PO to analyze scattering through an aperture. Figure 6 shows an electromagnetic plane wave which is incident normally on an aperture in a conducting screen of infinite extent. While this problem may not be realistic, it can make a good approximation for an aperture in an electrically large conductive plane. From the equivalence principle, the reradiated field appears to be generated by the current sheets described in Eq. (8). Starting from Maxwell's equations, the electric and magnetic fields radiated from the electric and magnetic current sources are (22)

$$\boldsymbol{E} = -j\frac{\omega\mu}{4\pi}\iint_{S'} \boldsymbol{J}'\frac{e^{-j\beta R}}{R}\,dx'\,dz' - \boldsymbol{\nabla}\times\left(\frac{1}{4\pi}\iint_{S'}\boldsymbol{M}'\frac{e^{-j\beta R}}{R}\,dx'\,dz'\right) \tag{19a}$$

and

$$\boldsymbol{H} = -j\frac{\omega\epsilon}{4\pi}\iint_{S'}\boldsymbol{M}'\frac{e^{-j\beta R}}{R}\,dx'\,dz' + \boldsymbol{\nabla}\times\left(\frac{1}{4\pi}\iint_{S'}\boldsymbol{J}'\frac{e^{-j\beta R}}{R}\,dx'\,dz'\right) \tag{19b}$$

where the primed symbols refer to the source rather than the field. The equivalence principle allows the electric field in the aperture to be replaced by the magnetic current sheet $\boldsymbol{M}_s$ over a continuous conducting screen (7). The aperture is essentially shorted, which cancels $\boldsymbol{J}_s$. From image theory, it appears as though an identical image of $\boldsymbol{M}_s$ lay on the opposite side of the screen. Since these two current sheets nearly coincide, the entire problem can be replaced with $2\boldsymbol{M}_s$ at the aperture location, and no screen at all. Then Eq. (19b) becomes

$$\boldsymbol{H} = -j\frac{\omega\epsilon}{2\pi}\iint_{S'}\boldsymbol{M}'\frac{e^{-j\beta R}}{R}\,dx'\,dz' \tag{20}$$

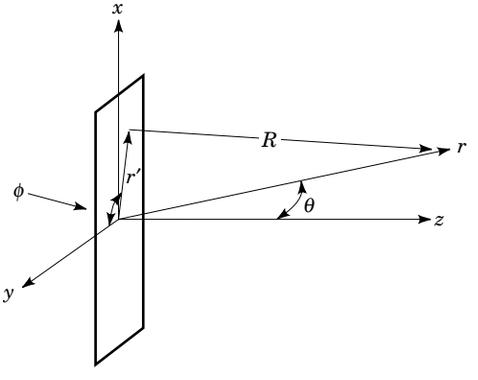

Figure 6. Coordinate system for the aperture diffraction problem. $\boldsymbol{R}$ is the vector pointing from the differential element $dx\,dy$ to the field point, and is the resultant vector sum of $\boldsymbol{r}$ and $\boldsymbol{r}'$. The distance from the origin to the secondary source in the aperture plane is $r' = \sqrt{x'^2 + y'^2}$.

Rather than solving the integrodifferential Eq. (19a), Ampere's law can be used to obtain directly the scattered electric field in the source-free region,

$$\boldsymbol{\nabla}\times\boldsymbol{H} = j\omega\epsilon\boldsymbol{E} \tag{21}$$

The distance R from each elemental source to the field point can be obtained from the law of cosines,

$$R = \sqrt{r^2 + r'^2 - 2rr'\cos\psi} \tag{22}$$

where $r'\cos\psi = x'\sin\theta\cos\phi + y'\sin\theta\sin\phi$. Equation (20) would be difficult to integrate with a direct substitution of Eq. (22). However, if the scattered field is observed in the far-field region, R and r will be virtually parallel. The far-field limit is usually taken to be

$$r \geq \frac{2D^2}{\lambda} \tag{23}$$

where D is the largest dimension of the aperture, in this case, the length of the diagonal (19). The far-field assumption allows for the approximation $R \approx r - r'\cos\psi$ in the phase, and $R \approx r$ in the amplitude. Furthermore, in the far field, $E = \eta H$, where $\eta = \sqrt{\mu/\epsilon}$ is the intrinsic impedance of the surrounding medium. This eliminates the need to solve Eqs. (19a) or (21). Since the incident plane wave is normal to the aperture, it will not vary over the aperture. Therefore, it can be brought out of the integral. Then the equation for the scattered magnetic field becomes

$$H = -j\frac{\omega\epsilon}{2\pi r}E_0\int_{-a/2}^{a/2}\int_{-b/2}^{b/2} e^{-j\beta(x'\sin\theta\cos\phi + y'\sin\theta\sin\phi)}\,dx'\,dz' \tag{24}$$

While appearing messy, Eq. (24) is a straightforward integral. After integrating the two exponential terms, substituting the limits, and applying the identity

$$\sin\alpha = \frac{e^{j\alpha} - e^{-j\alpha}}{j2}$$

the scattered magnetic field in Eq. (24) becomes

$$H = j\frac{abe^{-j\beta r}}{\eta\lambda r}\left(\frac{\sin X}{X}\right)\left(\frac{\sin Y}{Y}\right) \tag{25a}$$

where

$$X = \frac{\beta a\sin\theta\cos\phi}{2} \tag{25b}$$

and

$$Y = \frac{\beta b\sin\theta\sin\phi}{2} \tag{25c}$$

Figure 7 is a plot of Eq. (25a), with the amplitude normalized. The x dimension is $a = 6\lambda$, the y dimension is $b = 3\lambda$, and the observation screen is $z = 100\lambda$ from the aperture.

The normal incidence was chosen for this problem to illustrate the concept while keeping the mathematics simple.

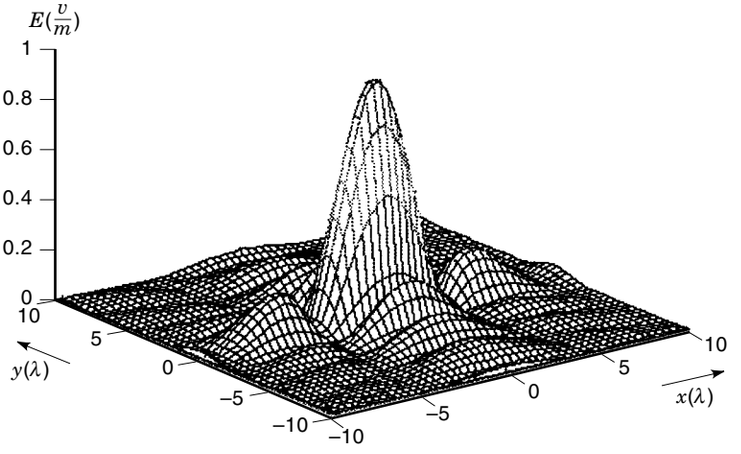

Figure 7. Normalized scattering pattern through the aperture. The dimensions of the aperture are 6 by 3 wavelengths; the observation screen is 100 wavelengths from the plane of the aperture. The scattering pattern is wider in the x direction, since the x dimension of the aperture is twice the y dimension.

However, Eq. (25) can be extended to oblique incidence by modifying the current source $\boldsymbol{M}_s$. Assuming that the source of the incident field is far from the aperture, the amplitude will not vary significantly across the aperture. However, the phase of each differential element of $\boldsymbol{M}_s$. will vary. The procedure is the same as for this analysis, except that some angle terms for the incident field will be added to X and Y in Eq. (25). The integration then follows in a similar manner (22).

BABINET'S PRINCIPLE

Scattering from a conductive plate can be modeled in a manner that virtually parallels the preceding solution to the aperture. In the case of scattering from a conductive plate, the current sources are obtained using the induction theorem. In fact, scattering through the aperture is the exact complement to the scattering off of the conductive plate that was essentially cut out of the conductive screen to create the aperture. If every electric parameter and the corresponding magnetic parameter were swapped, the solutions would be identical. Babinet's principle originally stated that the sum of the intensities from an obstruction and its complement (i.e., a similarly shaped aperture in an infinite screen) is equal to the intensity that would have existed if no obstruction existed at all:

$$S_a + S_c = S_0 \tag{26}$$

While this relationship works for optics, it does not take account of polarization. To apply Babinet's principle to vector fields, it must be modified to (23)

$$\frac{H^a}{H^i} + \frac{E^c}{E^i} = 1 \tag{27}$$

The first term in Eq. (27) is the ratio of the field diffracted by the aperture to the field with no screen present at all, and the second term is the ratio of the field produced by the complementary screen to the conjugate source. The conjugate source refers to the opposite field rotated by 90°. In vector form, Eq. (27) can be rewritten as

$$E^c = E^i - \eta H^a \tag{28}$$

which indicates that the electric field scattered from a conductive plate can be calculated from the field scattered from the aperture, by subtracting the latter from the incident field (22).

SPECIAL CASES OF ELECTROMAGNETIC WAVE SCATTERING

Rayleigh Scattering

If the scattering object is much smaller than a wavelength, its scattered energy varies inversely as the fourth power of the wavelength (1,24,25). Therefore, for a given subwavelength object, higher frequencies will scatter more than lower frequencies. This is the basis behind the concept of Rayleigh scattering for small scatterers. In fact, Rayleigh scattering answers the commonly asked question: Why is the sky blue? Since the blue end of the visible spectrum has the shortest wavelength, blue light scatters more than the rest of the visible spectrum from dust, water, and even air molecules. As the scattering objects become larger, they fall into the category called Mie scattering.

Radar Cross Section

Electromagnetic wave scattering is the basis by which radar signals are returned to the radar receiver from a target. Since the typical radar system employs a colocated transmit and receive antenna, the source and observation points are the same. This scenario is a specific case of electromagnetic wave scattering, as previously discussed, and is known as monostatic scattering.

As the transmitted power P_t propagates through space, it spreads over an increasing surface area, A, resulting in decreased power density $S_t = P_t/A$. If P_t spreads spherically, as with a point source or isotropic radiator, $A = 4\pi d^2$, where d is the distance from the transmitter. A target can intercept part of the transmitted power and scatter it in various directions. The radar cross section (RCS) is the effective area of the target that would return the monostatic power density back to the source, if this target scattered the power isotropically (1,26,27). The RCS is related to the physical cross-sectional area of the target but also depends on factors such as the frequency and polarization of the radar signal as well as the target's shape, material, and orientation to the transmitter.

SUMMARY

Since electromagnetic scattering perturbs the incident field, it can create interference, both constructive and destructive. The three main mechanisms of scattering are reflection, refraction, and diffraction. Reflection and refraction are the most common, and since these scattering mechanisms tend to be specular, they are easiest to analyze. Diffraction is much more difficult to analyze, and is typically not as dominant as the other two.

Various approximations can lead to solutions of diffraction problems. The two main approximations covered were the GTD, which takes advantage of ray tracing, and PO, which relies on the Huygens secondary sources. Slight modifications to the PO solution for the aperture problem can lead to solutions for backscattering and forward scattering from a conductive plate. This simple structure can serve as a building block for more complicated structures, which can be modeled as composites of conductive plates.

BIBLIOGRAPHY

1. J. D. Kraus, *Antennas,* 2nd ed., New York: McGraw-Hill, 1988.
2. C. R. Paul and S. A. Nasar, *Introduction to Electromagnetic Fields,* New York: McGraw-Hill, 1987.
3. C. T. A. Johnk, *Engineering Electromagnetic Fields and Waves,* New York: Wiley, 1988.
4. G. G. Skitek and S. V. Marshall, *Electromagnetic Concepts and Applications,* Englewood Cliffs, NJ: Prentice-Hall, 1982.
5. P. A. Tipler, *Physics,* New York: Worth, 1976.
6. C. A. Balanis, *Advanced Engineering Electromagnetics,* New York: Wiley, 1989.
7. E. C. Jordan and K. G. Balmain, *Electromagnetic Waves and Radiating Systems,* Englewood Cliffs, NJ: Prentice-Hall, 1968.
8. R. F. Harrington, *Time-Harmonic Electromagnetic Fields,* New York: McGraw-Hill, 1961.
9. G. E. Corazza et al., A characterization of indoor space and frequency diversity by ray-tracing modeling, *IEEE J. Selected Areas Commun.,* **14** (3): 411–419, 1996.
10. M. Kimpe, V. Bohossian, and H. Leib, Ray tracing for indoor radio channel estimation, *IEEE Proc. 2nd Int. Conf. on Universal Personal Commun. (ICUPC),* October 1993, pp. 64–68.
11. J. B. Keller, A geometric theory of diffraction, in L. M. Graves (ed.), *Calculus of Variations and its Applications, Proc. Symp. Appl. Math., Vol. III,* New York: McGraw-Hill, 1958, pp. 27–52.
12. G. E. Athanasiadou, A. R. Nix, and J P. McGeehan, Indoor 3D ray tracing predictions and their comparison with high resolution wideband measurements, *Proc. IEEE 46th Veh. Tech. Conf.,* April 1996, Vol. 1, pp. 36–40.
13. O. Landron, M. J. Feuerstein, and T. S. Rappaport, A comparison of theoretical and empirical reflection coefficients for typical exterior wall surfaces in a mobile radio environment, *IEEE Trans. Antennas Propag.,* **44**: 341–351, 1996.
14. R. H. Clarke and J. Brown, *Diffraction Theory and Antennas,* New York: Wiley, 1980.
15. J. D. Kraus, *Electromagnetics,* 4th ed., New York: McGraw-Hill, 1992, pp. 622–627.
16. R. G. Kouyoumjian and P. H. Pathak, A uniform geometrical theory of diffraction for an edge in a perfectly conducting surface, *Proc. IEEE,* **62**: 1448–1461, 1974.
17. J. B. Keller, Geometrical theory of diffraction, *J. Opt. Soc. Amer.,* **52** (2): 116–130, 1962.
18. J. B. Keller and Albert Blank, Diffraction and reflection of pulses by wedges and corners, in *The Theory of Electromagnetic Waves,* New York: Interscience, 1951, pp. 139–158.
19. C. A. Balanis, *Antenna Theory, Analysis and Design,* New York: Harper & Row, 1982, pp. 92–94, 448.
20. E. Hecht, *Optics,* 2nd ed., Reading, MA: Addison-Wesley, 1987, p. 393.
21. M. Spiegel, *Advanced Mathematics for Engineers and Scientists,* New York: McGraw-Hill, 1971.
22. R. L. Musselman, *Analytic non-asymptotic model for diffraction from large walls consisting of complex-shaped conductive scatterers,* Univ. Colorado, Colorado Springs, 1997.
23. H. G. Booker, Slot aerials and their relation to complementary wire aerials, *J. Inst. Electr. Eng., Part III A,* 1946, pp. 620–626.
24. A. Ishimaru, *Wave Propagation and Scattering in Random Media,* San Diego, CA: Academic Press, 1978.
25. H. C. van de Hulst, *Light Scattering by Small Particles,* New York: Dover, 1981.
26. M. I. Skolnik, *Introduction to Radar Systems,* 2nd ed., New York: McGraw-Hill, 1980.
27. S. A. Hovanessian, *Radar System Design and Analysis,* Norwood, MA: Artech House, 1984.

RANDALL L. MUSSELMAN
United States Air Force Academy